J Mater Sci (2010) 45:936–945
DOI 10.1007/s10853-009-4023-5

Novel approach for measuring the effective shear modulus of porous materials

Andrey V. Pyatigorets · Joseph F. Labuz · Sofia G. Mogilevskaya · Henryk K. Stolarski

Received: 17 August 2009 / Accepted: 5 November 2009 / Published online: 24 November 2009

Abstract A new approach is proposed for the experimental study of the effective shear modulus of porous elastic materials using the uniaxial tension test. The idea is to measure strains at a few points surrounding a cluster of holes that represents the structure of the material. The representative cluster is placed in the material with the same elastic properties as those of the matrix. The measured strains lead to the properties of the equivalent circular inhomogeneity, which would produce the same elastic fields as from the cluster. An aluminum plate containing a cluster of seven circular or hexagonal holes was used. The effective shear modulus obtained from the strain data was compared with theoretical predictions and various bounds, and it was shown that the laboratory estimated values are quite accurate. The experimental technique can be used for the determination of the effective Poisson's ratio of porous media and/or cellular solids if more detailed strain data are obtained.

Introduction

The problem of determining effective elastic properties of inhomogeneous (composite) materials has received much attention from researchers, who have proposed various micro-mechanical models and approximate solutions [1–4]. Many of these models admit different forms depending on whether particulate (three-dimensional case) or fibrous (two-dimensional case) composites or porous media are considered. Despite the number of different theoretical approaches, not much experimental work related to the study of the effective elastic properties, especially effective shear modulus and Poisson's ratio, of porous media can be found in the literature.

The majority of the existing experimental studies employ the concept of representative volume element (RVE), which has to be large enough in comparison to typical dimensions of the inhomogeneities to be characterized by the same overall mechanical properties as the whole material. In this context, Carvalho and Labuz [5] studied the dependence of the effective Young's modulus of plates containing randomly distributed slots or circular holes from the crack density or porosity, respectively. They observed the dependence of the results on the number of cracks or holes cut in the plates (for the same porosity or crack density) and also the dependence on whether cracks or holes were cut outside of the RVE. This suggests that the proper size of the RVE and proper boundary conditions are critical for the accurate determination of the effective properties of porous media. Lobb and Forrester [6] tested square metal sheets containing 3298 randomly distributed overlapping holes, and it was clear that application of proper boundary condition to the RVE was important (see discussion in [7]).

If the material possesses certain symmetry, the concept of a Representative Unit Cell (RUC) is often used, and it has been of great value for analytical and numerical analysis of composites [8, 9]. This concept, however, cannot be employed in experimental studies due to the technical difficulties of implementing the proper boundary conditions at the unit cell.

A. V. Pyatigorets (✉) · J. F. Labuz · S. G. Mogilevskaya · H. K. Stolarski
Department of Civil Engineering, University of Minnesota, Minneapolis, MN 55455, USA
e-mail: pyati002@umn.edu

Among other methods often used for the experimental studies of composite and porous media, the one that should be mentioned is based on the measurements of longitudinal and shear velocities of ultrasonic waves [10, 11]. This method is applied to bulk three-dimensional materials containing randomly distributed inhomogeneities and/or pores of microscopic sizes and relies on accurate measurements of the density and the waves' travel times.

The objective of this work is to present a new experimental methodology for determining the effective elastic properties of porous two-dimensional materials. The method employs the concept of a representative pattern [12] and, thus, does not have limitations inherent to the RVE and RUC, i.e., the necessity to provide proper boundary conditions. For many isotropic two-dimensional composites, the representative pattern is much smaller by size than the corresponding RVE. This feature allows for a more efficient design of specimens by using a smaller amount of inhomogeneities. For example, a plate with only seven holes placed in hexagonal arrangement is used in this study, while the minimum amount of holes in a rectangular RVE corresponding to the same geometry is 17, and additional holes have to be drilled outside the RVE to provide proper boundary conditions.

The theory used for problem analysis is presented in "Theoretical background". Section "Error estimation" is devoted to basic error analysis that is necessary for the efficient design of the experimental setup. The description of the setup and the specimen is given in section "Experiments," which is also devoted to the calculations of the elastic properties of the intact specimen. "Results and discussion" highlight the comparison with some existing analytical and numerical solutions. Several closing remarks along with some guidelines for new experiments are discussed in the conclusion.

Theoretical background

The proposed experimental procedure is based on the method of an equivalent inhomogeneity [12], which is similar in a broad sense to Saint-Venant's principle in relation to the effective properties of composite media. The method employs the concept of a representative pattern (Fig. 1a, b) that is used to represent the structure of a composite material. The concept of a representative pattern does not fully comply with the concept of a representative unit cell or representative volume element. The basic idea of the method is to construct a circular inhomogeneity in an infinite plane (Fig. 1c, d) whose effects on the elastic fields at distant points are the same as those of a finite cluster of inhomogeneities arranged in a pattern that represents the composite material in question. The mechanical properties of the equivalent inhomogeneity correspond to the effective properties of the composite material. The method works equally well for isotropic composites with periodic and random structures.

In order to determine the mechanical properties of the equivalent inhomogeneity, values of elastic fields at a few points located at some distance away from the cluster must be obtained. The proposed experimental procedure employs the measurements of strains at a few points surrounding the representative cluster of holes, which may be of any shape including elliptical holes and cracks (slots). The idea of the proposed method and the geometry of the problem are presented in Fig. 1.

Using the plane stress solution for a single circular elastic inhomogeneity embedded in an infinite elastic plane [13, 14], and assuming that the fields from the inhomogeneity and from the cluster of holes are the same at the point of measurement, it can be shown [13] that strains at this point are given by:

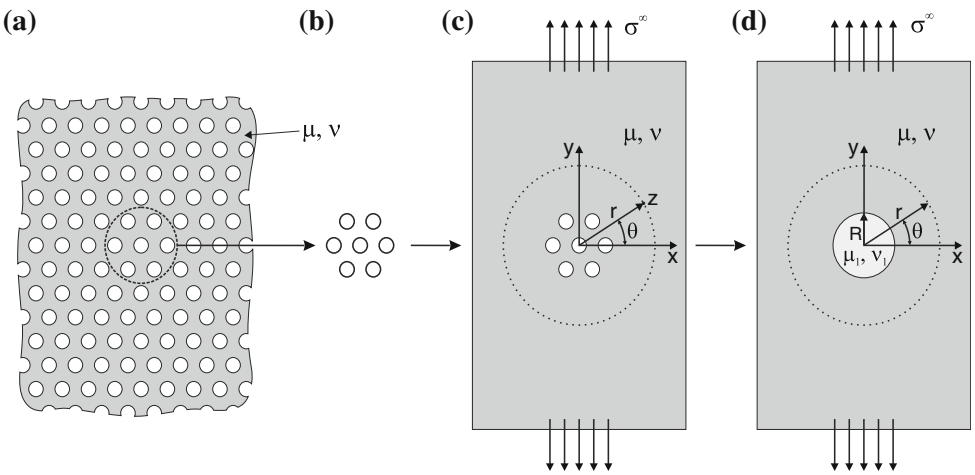

Fig. 1 The geometry of the problem. **a** Porous infinite plate. **b** Representative cluster. **c** Representative cluster of holes in a plate with the same properties as the original material. **d** Equivalent inhomogeneity

$$\varepsilon_{xx}+\varepsilon_{yy}=\frac{1-\nu}{1+\nu}\frac{\sigma^{\infty}}{2\mu}\left[\frac{\tilde{\mu}-1}{\tilde{\mu}+k}\frac{R^2}{r^2}\cdot 2\cos(2\theta)+1\right],$$
$$\varepsilon_{yy}-\varepsilon_{xx}+2i\varepsilon_{xy}=\frac{\sigma^{\infty}}{2\mu}\left[\frac{\tilde{\mu}-1}{\tilde{\mu}+k}\left(3\frac{R^2}{r^2}-2\right)\frac{R^2}{r^2}e^{-4i\theta}+\frac{\tilde{\mu}(\kappa_1-1)-(\kappa-1)}{\tilde{\mu}(\kappa_1-1)+2}\frac{R^2}{r^2}e^{-2i\theta}+1\right]. \quad (1)$$

Here $\tilde{\mu}=\mu/\mu_1$, μ and μ_1 are the shear moduli of the matrix and the equivalent inhomogeneity correspondingly, ν and ν_1 are Poisson's ratios of the matrix and the inhomogeneity correspondingly, $\kappa_1=(3-\nu_1)/(1+\nu_1)$ is the Kolosov–Muskhelishvili's parameter for the inhomogeneity, σ^{∞} is the uniform far-field stress applied to the plane, R is the radius of the inhomogeneity, and (r, θ) are polar coordinates of the point of measurement. Following the definition of volume fraction provided by Mogilevskaya et al. [12], the radius of the equivalent inhomogeneity can be expressed as:

$$R=\sqrt{\frac{S_{\text{void}}}{\pi n}}, \quad (2)$$

where S_{void} is the area occupied by voids in the representative cluster and n is porosity.

Experimental measurements were conducted within a polar coordinate system (i.e., components of ε_{rr} and $\varepsilon_{\theta\theta}$ were measured), therefore expressions 1 were transformed to polar coordinates as:

$$\varepsilon_{rr}+\varepsilon_{\theta\theta}=\varepsilon_{xx}+\varepsilon_{yy},$$
$$\varepsilon_{\theta\theta}-\varepsilon_{rr}+2i\varepsilon_{r\theta}=(\varepsilon_{yy}-\varepsilon_{xx}+2i\varepsilon_{xy})\cdot e^{2i\theta}. \quad (3)$$

Combining Eqs. 1 and 3 and extracting the real part, the following relations containing strain components ε_{rr} or $\varepsilon_{\theta\theta}$ were obtained:

$$\underbrace{\left[\frac{4\varepsilon_{\theta\theta}\mu}{\sigma^{\infty}}-\frac{1-\nu}{1+\nu}-\cos(2\theta)\right]\frac{r^2}{R^2}}_{y_{\theta\theta}}=\underbrace{\frac{\tilde{\mu}-1}{\tilde{\mu}+k}}_{a}\underbrace{\left[\frac{3}{2}\frac{R^2}{r^2}+\frac{1-\nu}{1+\nu}-1\right]2\cos(2\theta)}_{x_{\theta\theta}}+\underbrace{\frac{\tilde{\mu}(\kappa_1-1)-(\kappa-1)}{\tilde{\mu}(\kappa_1-1)+2}}_{b}$$
$$\underbrace{\left[-\frac{4\varepsilon_{rr}\mu}{\sigma^{\infty}}+\frac{1-\nu}{1+\nu}-\cos(2\theta)\right]\frac{r^2}{R^2}}_{y_{rr}}=\underbrace{\frac{\tilde{\mu}-1}{\tilde{\mu}+k}}_{a}\underbrace{\left[\frac{3}{2}\frac{R^2}{r^2}-\frac{1-\nu}{1+\nu}-1\right]2\cos(2\theta)}_{x_{rr}}+\underbrace{\frac{\tilde{\mu}(\kappa_1-1)-(\kappa-1)}{\tilde{\mu}(\kappa_1-1)+2}}_{b}. \quad (4)$$

Relations 4 are linear of the type $y=ax+b$. As soon as y and x are evaluated, the unknown parameters a and b can be easily found by using least squares fitting. Finally, the shear modulus of the equivalent inhomogeneity is found from parameter a, and the effective Poisson's ratio follows from the expression for parameter b.

Error estimation

Due to the fact that parameters $y_{\theta\theta}$ and y_{rr} in Eq. 4 depend on the values of strains $\varepsilon_{\theta\theta}$ and ε_{rr} measured experimentally, it is worth estimating at what locations r and θ the measurements would be the most accurate, so the error in $y_{\theta\theta}$ and y_{rr} would be minimal. Other parameters, namely shear modulus, Poisson's ratio, and applied stress, cannot be varied to reduce the error in expressions 4, thus they are considered to be fixed.

Assume that $\varepsilon_{\theta\theta}$, ε_{rr}, r, and θ contain errors:

$$\tilde{\varepsilon}_{rr}=\varepsilon_{rr}+\Delta\varepsilon_{rr},$$
$$\tilde{\varepsilon}_{\theta\theta}=\varepsilon_{\theta\theta}+\Delta\varepsilon_{\theta\theta},$$
$$\tilde{r}=r+\Delta r,$$
$$\tilde{\theta}=\theta+\Delta\theta, \quad (5)$$

where Δ represents the absolute error, which may be positive or negative. It turns out that the maximum absolute errors of $\tilde{y}_{\theta\theta}=y_{\theta\theta}\pm|\Delta y_{\theta\theta}|$ and $\tilde{y}_{rr}=y_{rr}\pm|\Delta y_{rr}|$ are the same and expressed as

$$|\Delta y_{kk}|\cong\left[\frac{2\mu}{\sigma^{\infty}}|\Delta\varepsilon_{kk}|+|\Delta\theta\sin(2\theta)|\right]\frac{2r^2}{R^2}+2|y_{kk}|\cdot|\Delta r/r|+\text{H.O.T.},\quad k=r,\theta \quad (6)$$

where H.O.T. stands for higher order terms.

It is expected that the error of strain measurements is the largest, and it can be shown that the first term in Eq. 6 contributes larger error than the second term. Thus, it follows from Eq. 6 that the closer the strains are measured to the cluster, i.e., the smaller r is, the smaller error $|\Delta y_{kk}|$ will be. However, at very small distances the cluster of inhomogeneities cannot be considered as a single equivalent inhomogeneity. Numerical simulations conducted by Mogilevskaya et al. [12] show that the minimal distance

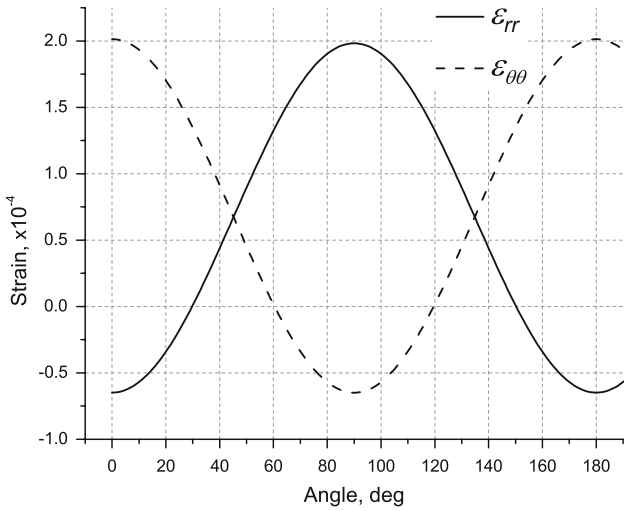

Fig. 2 Strain variation along a circle with radius r = 101.6 mm (4 in.) in an infinite plate with the representative cluster of holes

at which it is still possible to determine accurately the properties of the equivalent inhomogeneity is twice the size of the cluster. Therefore, it is reasonable to measure strains at the distances larger than $2r$.

As Eq. 6 depends on $\sin(2\theta)$, the choice of angles close to 0° or 90° provides the smallest error $|\Delta y_{kk}|$. Moreover, numerical modeling of strain fields for an infinite plane containing a hexagonal cluster of circular holes (as in Fig. 1c) reveals that the highest magnitude of radial and circumferential strains is reached at the same angles (see Fig. 2). Thus, the preferable location of sensors for measuring strain should be close to 0°, 90°, 180°, and 270°.

The plots in Fig. 2 are obtained with the use of the method described in [15]. The geometry of the solved problem is as follows: the holes are arranged in a hexagonal pattern (as in Fig. 1c); the diameter of each hole is $d = 10.1$ mm and the distance between the centers of the holes is $l = 15.2$ mm; the Young's modulus of the material $E = 72$ GPa and its Poisson's ratio is $\nu = 0.33$ (these values correspond to average values of aluminum); stress $\sigma^{\infty} = 14.5$ MPa is applied along the y-axis (as in Fig. 1c); strains are measured along the circle with radius $r = 101.6$ mm, which is approximately four times larger that the size of the cluster of holes.

The maximum absolute error of $\tilde{x}_{\theta\theta} = x_{\theta\theta} \pm |\Delta x_{\theta\theta}|$ and $\tilde{x}_{rr} = x_{rr} \pm |\Delta x_{rr}|$ corresponding to Eq. 5 is found as

$$|\Delta x_{kk}| \cong 6\frac{R^2}{r^2}|\cos(2\theta)| \cdot |\Delta r/r| + 3\frac{R^2}{r^2}|\Delta\theta\sin(2\theta)| + \text{H.O.T.}, \quad k = r, \theta \tag{7}$$

In this case, the error is inversely proportional to r^2. However, both terms (R^2/r^2) are multiplied by small quantities $|\Delta r/r|$ and $|\Delta\theta\sin(2\theta)|$, values of which can be effectively controlled. Thus, the assumption that more accurate measurements can be obtained at smaller r remains valid.

It is necessary to note that expression 2 is not exact due to the fact that the definition of the volume fraction given in the method of an equivalent inhomogeneity differs from the conventional definition. However, as it was shown by Mogilevskaya et al. [12], the results for effective elastic moduli found with the use of either of these definitions are almost identical. Therefore, the conventional definition for volume fraction (porosity) can be used to calculate the radius of the equivalent inhomogeneity R.

Experiments

The main purpose of this paper is to provide an experimental approach for determining the effective shear modulus of isotropic elastic porous materials. The present work is particularly devoted to the study of infinite sheets perforated with circular or hexagonal holes that are uniformly distributed in a hexagonal arrangement. The minimal representative cluster of such a material consists of seven holes (see Fig. 1a, b). The testing was accomplished by subjecting an elastic plate containing such a representative cluster of holes to uniaxial tensile stress under plane stress conditions.

Despite the fact that the mechanical properties of the material under consideration do not depend on the direction of loading, numerical modeling revealed that stresses locally depend on the direction of the applied load. Figure 3 shows that the magnitude of major principal stress is higher at certain locations for the case when the load is applied along the closest packing direction (CPD, Fig. 3b) in comparison with the case when it is applied in the direction of mid-closest packing (mid-CPD, Fig. 3a). In order to prevent any local yielding, it is convenient to choose the position of holes at which the smaller local stresses occur. It is seen from Fig. 3 that for a material with Young's modulus $E = 72$ GPa and Poisson's ratio $\nu = 0.33$, major principal stress reaches the value of 105 MPa when far field stress $\sigma^{\infty} = 25$ MPa is acting in CPD, and it is below 95 MPa when the load is applied along mid-CPD. Both of these values are well below the plastic yield limit $\sigma_Y = 270$ MPa. Nevertheless, the configuration corresponding to the load application along mid-CPD was chosen for experiments. Figure 3 is plotted for the case when the diameter of holes is $d = 10.1$ mm and the distance between their centers is $l = 15.2$ mm. In order to investigate the stress distribution in specimens with higher porosity, similar modeling was conducted. In this case, the diameter of the holes $d = 13$ mm and far field stress $\sigma^{\infty} = 25$ MPa was applied along mid-CPD. It was found that maximum principal stress does not exceed

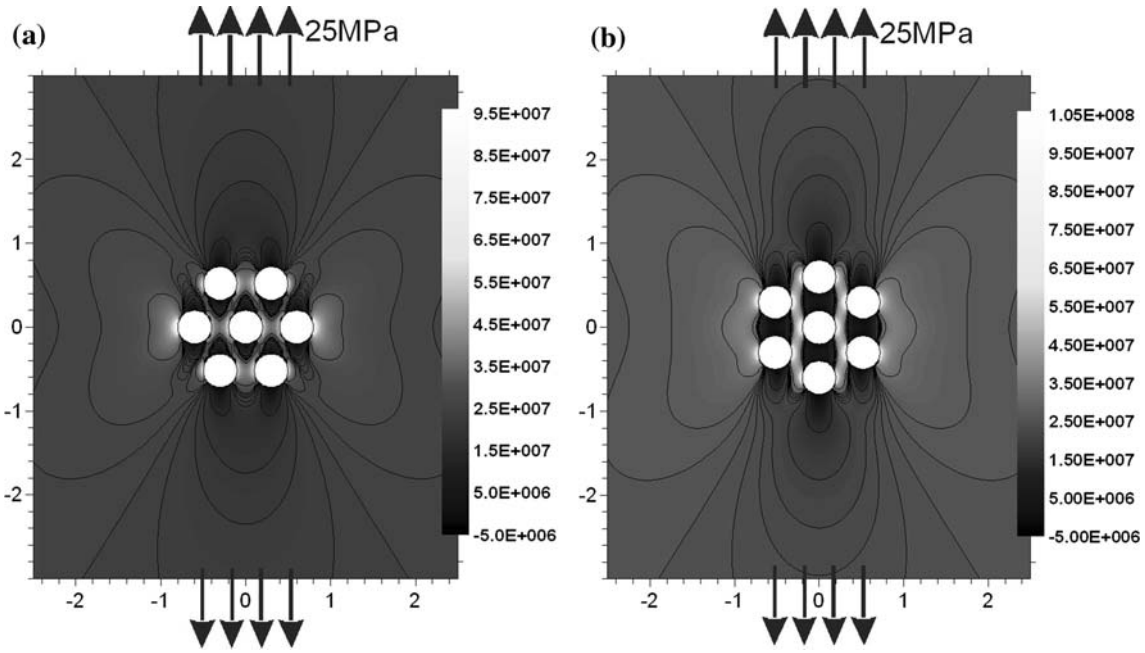

Fig. 3 Distribution of major principal stress in an infinite plate with a representative cluster of holes. Far field stress is applied along **a** mid-closest packing direction (mid-CPD), **b** closest packing direction (CPD). Dimensions are given in inches

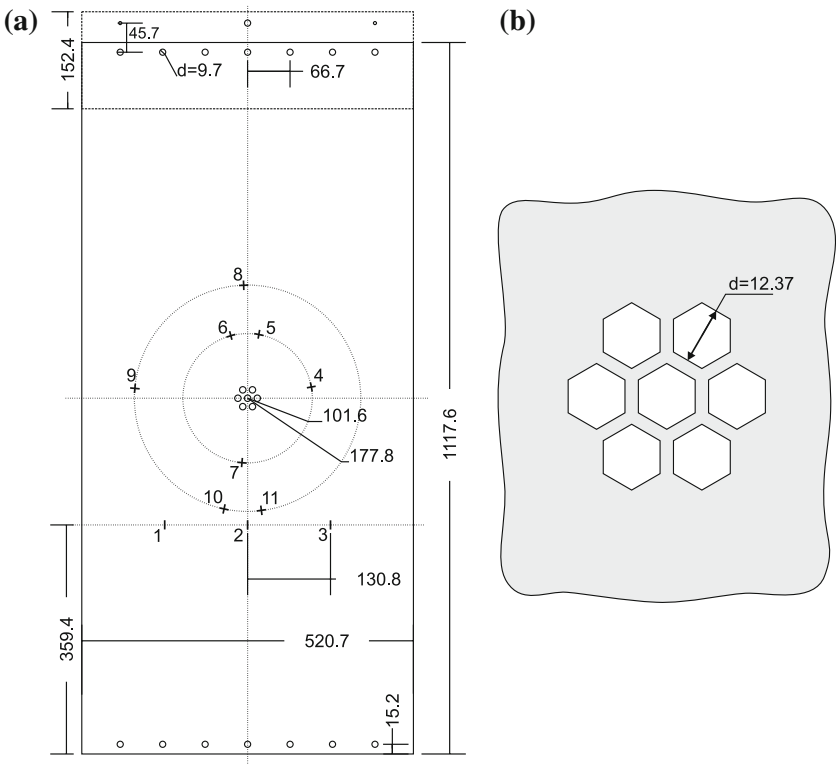

Fig. 4 **a** Geometry of the specimen. Steel reinforcing plates are shown on the top part of the figure by the dashed line. **b** The dimensions of the largest hexagonal holes cut in the plate. Dimensions are given in millimeters

104 MPa and it localized at the sides of the most right and the most left holes (as in Fig. 3a). The stress does not increase significantly between the holes due to their shielding effect on each other.

The specimen used in the series of experiments was a rectangular aluminum (alloy 6061) plate with the dimensions presented in Fig. 4a (all dimensions in Fig. 4 are given in millimeters). The plate was 1.6 mm (0.063 in.)

thick, with a plane area 1117.6 mm × 520.7 mm (44 in. × 20.5 in.). During the tests, the plate was pulled in tension along its length. In order to provide uniform loading, the aluminum plate was connected to steel reinforcing plates through a set of holes drilled at the lower and upper ends (Fig. 4). The thickness of the reinforcing plates was 1.6 mm, and they were attached to the aluminum plate from the front and back (in total four steel plates were used) by a system of steel pins of approximately the same diameter as the holes ($d = 9.7$ mm). The reinforcing plates then were loaded through a single hole with diameter $d = 9.7$ mm by a steel dowel. All the holes were located and drilled within the accuracy of at least 0.1 mm. For better alignment, two additional holes of smaller diameter were drilled in the steel plates and then were tightened with bolts.

In order to check the homogeneity of the stress distribution across the specimen, three linear strain gages were attached at approximately one third of the distance between the arrays of holes. These strain gages are numerated by 1, 2, and 3 in Fig. 4. One strain gage was glued along the middle line of the plate (gage # 2) and the other two were placed approximately in the middle of the right and left halves of the plate. All gages were placed at the same vertical position. The length of the strain gages was 3 mm, which provided minimal error in pointwise strain measurements. The resistance of the strain gages was 120 Ω ± 0.5 Ω, and their coefficient of thermal expansion was 23×10^{-6} °C^{-1}. Temperature effects were not an issue as the temperature was kept approximately constant around 21 °C throughout the whole series of experiments. A quarter Wheatstone bridge was used for measuring the change in resistance of the strain gages. The bridge was powered with 5 Volts, and the output was amplified so it varied in the range of ±1 V. Then the output was digitized with a 12 bit analog-to-digital converter (ADC), and data were recorded at an interval of 1 s.

First, the original plate without the representative cluster of holes was tested. It was found that the distribution of stresses along the testing region was approximately uniform, and the difference between the strains measured at the centerline of the plate and close to its edges was less than 3%. Monitoring of the uniformity of load distribution was also conducted during each test. The initial tests, conducted without reinforcing plates when only the central holes of the aluminum plate were loaded, revealed that the strain difference may be as high as 10–12% at the monitored region.

Eight T-rosette strain gages, placed at two circles of radii 101.6 and 177.8 mm surrounding the representative cluster of holes, were used to measure radial and circumferential strains in the plate. According to the error analysis presented, the location of strain gages was chosen to be close to 0°, 90°, 180°, and 270°. The exact location in a polar coordinate system is provided in Table 1 (the angles are calculated counterclockwise from the x-axis, as in Fig. 1c). The error with which the location of strain gages was determined was not more than $\Delta\theta = \pm 0.5°$ and $\Delta r = \pm 0.5$ mm. The technical parameters of the T-rosette strain gages correspond to those for the linear strain gages.

Table 1 T-rosette strain gages locations

Gage #	4	5	6	7	8	9	10	11
Angle θ from Ox	10°	80°	105°	265°	92°	175°	258°	277°
Radius	$r = 101.6$ mm				$r = 177.8$ mm			

The sensitivity of the load cell was 1.09 kN/mV, and the data were digitized with 12 bit ADC and recorded at an interval of 1 s. All recording devices were synchronized between each other and the error of synchronization did not exceed 1 s over 1 h time interval.

The size of the circular holes in the representative cluster corresponded to certain drill sizes. Each next set of holes was overdrilled from the previous set to increase the porosity of the representative cluster, while their location remained the same. Lastly, hexagonal openings were cut in the plate in place of circular holes. This geometry may be considered to be corresponding to honeycomb cellular solids, which was theoretically studied by various researchers (e.g. [16]). In total, four sets of holes and two sets of hexagonal openings were studied. Their sizes and corresponding porosity are given in Table 2.

For the case of hexagonal openings, the hole diameter in Table 2 means the distance between two opposite sides of the hexagon (Fig. 4b). The central hole was drilled in the geometrical center of the aluminum plate, and the position of its center was taken as the origin: $(x, y) = (0, 0)$. The distance between centers of other holes and the origin was 7.62 mm. The error in locating the holes did not exceed ±0.1 mm.

The Young's modulus of the intact plate was determined based on the readings from the three linear strain gages and far-field stress data, which were determined by dividing the applied load by the cross-sectional area of the plate (833.12 mm^2). The obtained value for the Young's modulus was $E = 67.9 \pm 0.1$ GPa.

The calibration tests revealed that the response was nonlinear for small load applied to the specimen. This is explained by the fact that the aluminum plate was slightly bent. Therefore, before starting any measurements, the

Table 2 Parameters of the openings

Porosity n, %	2.42	14.27	27.77	44.84	51.24	65.88
Hole diameter, mm	2.49	6.05	8.43	10.72	10.91	12.37
Hole type	Circular				Hexagonal	

specimen was preloaded to 5 kN. The measurements were then proceeded until the load reached 20 kN, and the readings were taken in real time. The specimen showed elastic behavior during the tests for the loads applied. The measurement were taken upon loading and unloading of the specimen and repeated four times for each porosity.

The stress–strain curves obtained for each strain gage were fitted by linear regression. The coefficient of determination (COD), or R^2, was between 0.995 and 1.0 for all fitted data, confirming that strain changed linearly with the load. Having stress–strain response for each data set, the value of load corresponding to 15 kN was used to obtain corresponding strains.

It was found that the readings from the strain gages located at the larger circle (r = 177.8 mm) contained significant errors and could not be used to provide accurate values for the elastic properties of the equivalent inhomogeneity. As these sensors are located closer to the plate edges, their strain readings are prone to larger errors due to the larger nonuniformity in stress distribution and edge effects. In addition, the values of strains obtained from the strain gages at the larger circle are much closer to the values of far-field state of strain, and may not represent well the effect of circular holes in the plate.

Results and discussion

Equation 4 was used to calculate the shear modulus μ_1 of the equivalent inhomogeneity and its Poisson's ratio ν_1. It is more convenient though, to use a slightly modified version of Eq. 4. Adding $x_{\theta\theta}$ and x_{rr} to the left-hand side and the right-hand side of the first and the second expressions 4 respectively, yields

$$\begin{aligned} y_{\theta\theta} + x_{\theta\theta} &= (a+1)x_{\theta\theta} + b, \\ y_{rr} + x_{rr} &= (a+1)x_{rr} + b, \end{aligned} \tag{8}$$

where $y_{\theta\theta}$, $x_{\theta\theta}$, y_{rr}, and x_{rr} are defined in Eq. 4. The values of independent variables ($x_{\theta\theta}$ and x_{rr}) and corresponding to them values of the left-hand side of Eq. 8 create a data set that needs to be sorted in ascending order before any least squares fitting can be done. The data from eight strain gages results in eight points in the data set for each value of r. Eq. 8 include the Poisson's ratio ν of the intact material, where $\nu = 0.315 \pm 0.003$ was found through numerical simulations using known (measured) Young's modulus $E = 67.9$ GPa and values of strains measured at several points.

For the case of $r = 101.6$ mm (smaller circle), plots corresponding to Eq. 8 are presented in Fig. 5. The lines are fitted by linear regression, and the parameters of fitting are given in Table 3. Effective shear modulus can be found from the slopes of the fitting functions, and the values are provided in Table 3. Due to the ability to simulate elastic fields in infinite media perforated with circular holes, this information can be used for the theoretical determination of the effective shear modulus, as it is described in [12]. These results are given in Table 3 for the first four porosities, which correspond to circular holes.

It can be seen from Table 3 that the slopes accurately define the effective shear modulus of the equivalent inhomogeneity. However, it was found that the data for the intercept b cannot provide accurate values for the effective Poisson's ratio. This is due to the fact that Poisson's ratio depends on both parameter b and the effective shear modulus, associated with some error (see Eq. 4). It follows from the results of numerical simulations that the accuracy of the determination of Poisson's ratio can be significantly increased if 19 holes are considered in the representative cluster (for the hexagonal arrangement) instead of seven holes, as in the present work. In other experimental studies, the effective Poisson's ratio is usually not measured directly, but rather expressed through the effective bulk and Young's moduli [17], which have to be measured very accurately to provide reasonable values for Poisson's ratio.

As expected, the effective shear modulus decreases as the porosity increases. The good match of experimental and numerically modelled data is evident. Some noticeable difference between experimental and theoretical predictions for the porosity n = 14.27% can be explained by the experimental errors (in this case some mechanical problems in the load frame were observed, which resulted in noticeable noise in load and strain measurements).

The results for the effective shear modulus given in Table 3 are compared (Fig. 6) with those obtained from the Differential Effective Medium (DEM) method [18], where a solution to the problem of cylindrical inhomogeneities randomly distributed in a transversely isotropic composite can be found. DEM results in a system of ordinary differential equations that can be solved analytically for the case of hollow cylinders to obtain the effective transverse shear modulus. The results obtianed with DEM agree well with the experimental results for small porosities.

The topmost graph in Fig. 6 represents the well known Hashin–Shtrikman upper bound on the effective shear modulus [19], obtained for the limiting case when the properties of one of the phases are equal to zero (voids). The corresponding lower bound is trivially zero. The Hashin–Shtrikman bounds for the effective shear modulus may be considered as the best possible bounds in terms of volume fraction [1]. These bounds, however, do not take into account the structure of the material and interactions between inhomogeneities. Nevertheless, for the case of the porous medium considered in the present work, the upper bound provides quite accurate results if compared with experimental (circles) and numerical (squares) data for

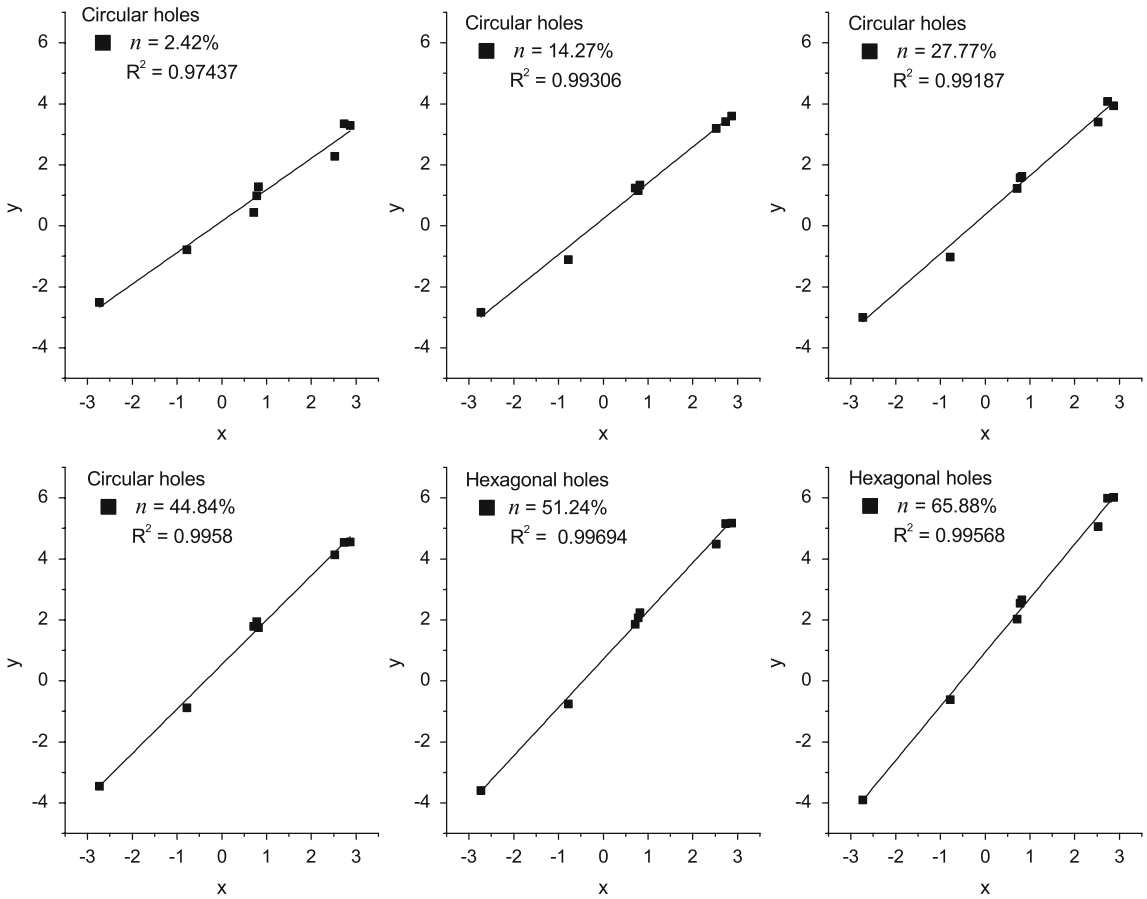

Fig. 5 Least squares fitting of experimental data (see Eq. 8)

Table 3 Fitting parameters for Eq. 8 for strains measured at the smaller circle (r = 101.6 mm)

Porosity n, %	Slope $(a + 1)$	Intercept (b)	R^2 (COD)	μ_1 (exp), GPa	μ_1 (theor), GPa	μ_1/μ (exp)	μ_1/μ (theor)
2.42	1.03144	0.14961	0.97437	23.49	24.01	0.91	0.93
14.27	1.17804	0.23102	0.99306	15.57	17.12	0.60	0.66
27.77	1.28168	0.36512	0.99187	11.77	11.68	0.46	0.45
44.84	1.4587	0.5353	0.9958	7.23	6.64	0.28	0.26
51.24	1.58252	0.70824	0.99694	4.93	–	0.19	–
65.88	1.77331	0.9362	0.99568	2.58	–	0.09	–

porosities below 50%. Besides, all results and the upper bound obtained for small porosities match dilute concentration results [20]. For larger porosities, the Hashin–Shtrikman upper bound diverges from the experimental data and high-concentration results obtained by Day et al. [7] for circular holes. It is seen from Fig. 6 that the Hashin–Shtrikman upper bound is not able to predict the percolation limit that occurs at 91% porosity for circular holes.

Lastly, experimental results are compared (Fig. 7) with highly-accurate numerical results obtained by Eischen and Torquato [9]. The authors exploited the concept of a representative unit cell and used the boundary element method to obtain effective elastic properties of porous plates. One of the examples provided by Eischen and Torquato (Table IX in [9]) is similar to the problem considered in the present work with the only difference that the Poisson's ratio of the matrix $\nu = 0.33$ was used in their work. Nevertheless, it is reasonable to compare the present results with those provided by Eischen and Torquato due to the following fact. Using the method of the equivalent inhomogeneity, it has been shown that the difference in the effective shear modulus for the cases when Poisson's ratio of the matrix is 0.315 or 0.33 is negligible (for example, compare the location of squares and solid line in Fig. 7),

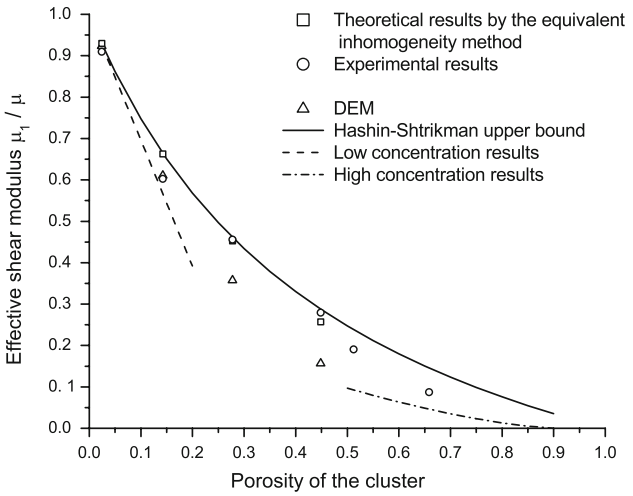

Fig. 6 Experimental results for the effective shear modulus in comparison with theoretical predictions. Squares correspond to numerically modelled data from Table 3

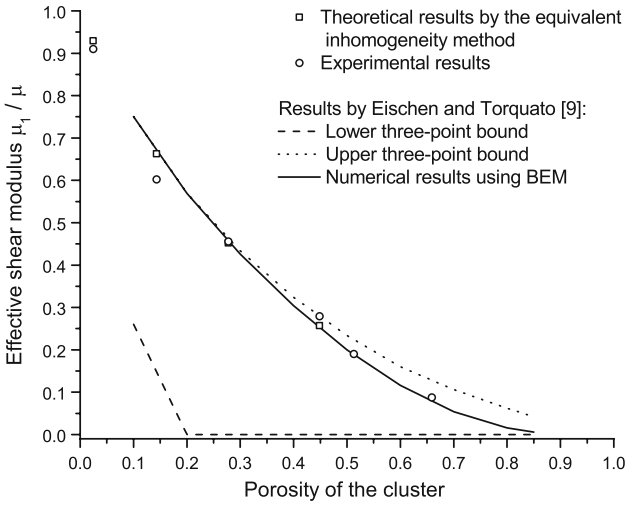

Fig. 7 Experimental results for the effective shear modulus in comparison with the results obtained by Eischen and Torquato [9]. Data from [9] are obtained for $\nu = 0.33$, while all other data in the figure are obtained for $\nu = 0.315$

and both of these results match closely the results of Eischen and Torquato. This allows for comparison of the experimental data with the results from [9], and the good agreement is shown in Fig. 7. It should be noted that the results from [9] were obtained for holes of circular shape. Thus, any data shown in Fig. 7 for the porosity $n > 0.5$ (except for the experimental results) should be considered as approximate.

Despite the fact that holes with circular and hexagonal shapes were studied in this work, the proposed experimental methodology can be used for the determination of the effective properties of porous materials containing holes of any shape or even cracks (slots). Their distribution can be periodic or random as long as the effect on the overall elastic moduli is isotropic. The most appropriate shape of the cluster appears to be circular since the method presented here is based on the analytic solution for a single circular inhomogeneity. However, other clusters with certain number of symmetries may be equally appropriate. This opinion is based on the work of Ekneligoda and Zimmerman [21], who discuss the issue of whether a single hole placed in an infinite elastic medium behaves isotropically. Theoretically, even a rectangular shape of the cluster can be used. For example, Mogilevskaya et al. [12] studied numerically the effective properties of porous media with a random distribution of circular holes. Only 34 holes were considered in the representative cluster, and the cluster had a square shape. The distances at which the values of elastic fields were found to compute effective properties were 50–70 times larger than the size of the cluster. However, from the experimental point of view, this is not practical because of the space limitations and loss of the measurement accuracy. In experiments, the strain measurements should be taken at much closer distances (2–4 times size of the cluster), thus the shape of the representative cluster is important. The choice of a nearly circular shape of the cluster ensures that the cluster behaves isotropically at small distances.

Conclusions

This paper is concerned with the experimental study of the effective shear modulus of porous materials based on the equivalent inhomogeneity method. According to the approach, a small representative cluster of inhomogeneities of the material is placed within the intact material with the same properties as those of the composite's matrix, and strains are measured around the cluster. The major advantage of the proposed experimental method is that there is no need to consider a representative volume element (RVE). Therefore, the number of holes in the representative cluster may be much smaller in comparison with the number of holes in the RVE.

It should be noted that the numerical simulations conducted to obtain the theoretical predictions cannot substitute for the experimental determination of the effective properties. This is due to the limitation of the numerical model dealing with circular holes only. Even if the elastic fields are simulated with other methods, e.g. finite element or boundary element methods, it is difficult to obtain accurate results for complex geometries (for example, multiple random cracks or cellular solids). Experiments can be conducted for the openings of any shape and any arrangements as long as the representative cluster is isotropic.

The effective shear modulus for the holes of circular and hexagonal shape has been accurately determined from the strain measurements conducted at the distance of about four times larger than the size of the cluster. The results were compared with the predictions from the Differential Effective Medium Model, low- and high-concentration approximations, and from numerical analysis. It was shown that experimental results lie between bounds and match the numerical results.

The measurements conducted at the distance seven times larger than the size of the cluster did not provide accurate strain data to calculate effective properties of the porous medium. The accuracy of the results can be increased if the measurements are taken closer to the cluster of the holes to avoid any effects connected with the finite size of the plate. Conducting measurements in such locations would also allow reducing the overall size of the specimen.

Acknowledgements Partial support for this work was provided by the National Science Foundation, Grant Number CMMI-0825454.

References

1. Hashin Z (1983) J Appl Mech 50:481
2. Christensen RM (1990) J Mech Phys Solids 38(3):379
3. Markov KZ, Preziosi L (2000) Heterogeneous media: micromechanics modeling methods and simulations. Birkhauser, Boston
4. Mishnaevsky L Jr (2007) Computational mesomechanics of composites: numerical analysis of the effect of microstructures of composites of strength and damage resistance. Wiley-Interscience, Chichester, UK
5. Carvalho FCS, Labuz JF (1996) Int J Solids Struct 33(28):4119
6. Lobb CJ, Forrester MG (1987) Phys Rev B 35(4):1899
7. Day AR, Snyder KA, Garboczi EJ (1992) J Mech Phys Solids 40(5):1031
8. Achenbach JD, Zhu H (1990) Trans ASME 57:956
9. Eischen JW, Torquato S (1993) J Appl Phys 74:159
10. Panakkal JP, Willems H, Arnold W (1990) J Mater Sci 25:1397. doi:10.1007/BF00585456
11. Sayers CM (1993) Ultrasound in solids with porosity, microcracking and polycrystalline structure. In: Achenbach JD (ed) Evaluation of materials and structures by quantitative ultrasonics. Springer, Wien
12. Mogilevskaya SG, Crouch SL, Stolarski HK, Benusiglio A (2009) Int J Solids Struct. doi:10.1016/j.ijsolstr.2009.10.007
13. Mogilevskaya SG, Crouch SL (2001) Int J Num Methods Eng 52:1069
14. Mogilevskaya SG, Crouch SL, Stolarski HK (2008) J Mech Phys Solids 56(6):2298
15. Wang J, Crouch SL, Mogilevskaya SG (2003) Eng Anal Bound Elements 27:789
16. Torquato S, Gibiansky LV, Silva MJ, Gibson LJ (1998) Int J Mech Sci 40(1):71
17. Phani KK, Sanyal D (2005) J Mater Sci 40:5685. doi:10.1007/s10853-007-1677-8
18. McLaughlin R (1977) Int J Eng Sci 15:237
19. Hashin Z (1965) J Mech Phys Solids 13:119
20. Chow TS, Hermans JJ (1969) J Compos Mater 3:382
21. Ekneligoda TC, Zimmerman RW (2008) Proc R Soc Lond Ser A 464:759